



## Effect of exogenous glutathione supplementation on the *in vitro* developmental competence of ovine oocytes

Jingyu Ren <sup>a</sup>, Yuchun Hao <sup>a</sup>, Zhanpeng Liu <sup>a</sup>, Shubin Li <sup>b</sup>, Chunyu Wang <sup>a</sup>, Biao Wang <sup>c</sup>, Yongbin Liu <sup>c</sup>, Gang Liu <sup>d,\*</sup>, Yanfeng Dai <sup>a,\*\*</sup>

<sup>a</sup> College of Life Science, Inner Mongolia University, 235 West Univ. Road, Hohhot, 010021, Inner Mongolia, China

<sup>b</sup> Department of Geriatric Medical Center, Inner Mongolia People's Hospital, 20 Zhaowuda Road, Hohhot, 010021, Inner Mongolia, China

<sup>c</sup> Animal Husbandry Institute, Inner Mongolia Academy of Agricultural & Animal Husbandry Sciences, 22 Zhaojun Road, Hohhot, 010031, Inner Mongolia, China

<sup>d</sup> Key Laboratory of Medical Cell Biology, Clinical Medicine Research Center, Affiliated Hospital of Inner Mongolia Medical University, 1 Tongdao North Street, Hohhot, 010050, Inner Mongolia, China

### ARTICLE INFO

#### Article history:

Received 30 December 2020

Received in revised form

22 July 2021

Accepted 24 July 2021

Available online 8 August 2021

#### Keywords:

Exogenous GSH

Reactive oxygen species

Ovine oocytes

IVM

Embryonic development

### ABSTRACT

The beneficial effect of glutathione (GSH) on the *in vitro* maturation (IVM) of bovine/porcine oocytes has been confirmed; however, the antioxidant effect of exogenous GSH supplementation on the IVM of ovine oocytes has not been determined. In this study, ovine cumulus oocyte complexes (COCs) were classified into three groups according to the layer number of cumulus cells (the Grade A group has more than five layers, the Grade B group has three to four layers and the Grade C group has less than three layers). After *in vitro* culture of COCs in the presence of exogenous GSH, the meiotic competence of ovine oocytes was assessed by analyzing nuclear maturation to metaphase II (MII) stage, cortical granules (CGs) dynamics, astacin like metalloendopeptidase (ASTL) distribution, histone methylation pattern, reactive oxygen species (ROS) production, mitochondrial activities and genes expression. After *in vitro* fertilization (IVF), assessments of embryonic development were conducted to confirm the effects of exogenous GSH supplementation. The results showed that exogenous GSH not only enhanced the maturation rates of the Grade B and Grade C groups but also promoted CGs dynamics and ASTL distribution of the Grade A, B and C groups ( $p < 0.05$ ). Exogenous GSH increased the mitochondrial activities of the Grade A, B and C groups and decreased the ROS production levels of oocytes ( $p < 0.05$ ), regardless of the layer number of cumulus cells. Moreover, exogenous GSH promoted the expression levels of genes related with oocyte maturation, antioxidant activity and antiapoptotic effects in the Grade B and Grade C groups ( $p < 0.05$ ). The expression levels of H3K4me3 and H3K9me3 in the Grade B and Grade C groups were promoted after exogenous GSH supplementation ( $p < 0.05$ ), consistent with the expression levels of genes related with histone methylation ( $p < 0.05$ ). In addition, exogenous GSH strongly promoted the embryonic developmental competence of Grade B and Grade C groups ( $p < 0.05$ ). Taken together, our findings provide foundational evidence for the free radical scavenging potential of exogenous GSH in the *in vitro* developmental competence of ovine oocytes, especially oocytes from COCs lacking cumulus cells. These findings, which demonstrated the potential for improving the quality of ovine oocytes during IVM, will contribute to researches on GSH applications and the efficiency of assisted reproductive technology for ovine breeding.

© 2021 Elsevier Inc. All rights reserved.

### 1. Introduction

According to the Data Retrieval Committee of the International Embryo Transfer Society (IETS), millions of animals, including bovines, horses, ovines and porcines, have been born via assisted reproductive technologies (ARTs) during the past decades, demonstrating the important role and safety of ARTs. In addition,

\* Corresponding author.

\*\* Corresponding author.

E-mail addresses: [21408010@mail.imu.edu.cn](mailto:21408010@mail.imu.edu.cn) (G. Liu), [daiyf@imu.edu.cn](mailto:daiyf@imu.edu.cn) (Y. Dai).

ARTs with ovine oocytes with commercial value or desirable genetic qualities obtained from slaughtered donors or donors with valuable genetic qualities significantly reduced the generation intervals by 5–6 months, promoted genetic gain and benefited subsequent ovine breeding [1–3].

Despite these promising achievements in research on ARTs for the *in vitro* production of embryos, both for human reproductive medicine [4] and the livestock breeding industry [5], the current microenvironments used for livestock IVM are still suboptimal compared with the *in vivo* microenvironments [6,7], regardless of the improved IVM efficiency achieved by the application of low oxygen incubators combined with endogenous or exogenous supplementation to the IVM system [8–10]. According to these previous studies, the excessive production of reactive oxygen species (ROS) and the resulting oxidative stress were negatively related to the efficiency of *in vitro* oocyte development [11–13]. The endogenous production and dynamic neutralization of ROS, which are strictly regulated by antioxidant defense systems, including endogenous superoxide dismutase (SOD), catalase (CAT), alkyl hydroperoxide reductase (AhpC) and the glutathione (GSH)-cycling system [14], play key roles in the regulation of cell fates, including proliferation, differentiation and apoptosis, via various signaling molecules and pathways. However, the excessive accumulation of ROS results in intracytoplasmic oxidative stress, affecting molecules, cell structures and protein functions. These changes also contribute to oocyte deteriorations, telomere shortening and zona pellucid hardening [15–17], possibly triggering reproductive diseases, pregnancy complications, infertility and abortions [18,19].

Moreover, the excessive accumulation of ROS and oxidative disturbances in postovulatory oocytes are believed to be responsible for the abnormal epigenetic alterations and chromosome non-dysjunction, further causing abnormal spindle formation, chromosomal misalignment and aneuploidy [20–25]. As a necessary regulator for oocyte maturation, epigenetic modifications regulated the structure of histone and DNA, in turn affecting the gene expression. The epigenetic alterations of DNA methylation and histone methylation have been proved with potential damages to mammalian oocyte development [24].

In addition, histone methylation, tightly regulated by histone lysine methyltransferases (such as KMT2b) and histone lysine demethylases (such as KDM1a, KDM1b, KDM4d and KDM5b), has been proved as the major determinant for the formation of transcriptionally active and inactive regions of the genome, and the former studies have found that histone methylations including H3K4me3 and H3K9me3 not only regulate oocyte development, also play crucial roles in the following zygotic genome activation (ZGA) and maternal-to-zygotic transition (MZT) after fertilization [26–29].

In fact, several literatures have confirmed the beneficial role of reducing ROS accumulation related oxidative disturbance and abnormal histone methylation level at the same time on the IVM of mammalian oocytes [21,30], further revealing the hypothesis that the IVM supplementation with dual potentials of decreasing abnormal histone methylation levels and reducing ROS accumulation will benefit the IVM of ovine oocytes.

GSH, a tripeptide synthesized from glycine, cysteine and glutamate, is the most important redox-regulating nonenzymatic thiol for the regulation of ROS production and defence against oxidative stress-related damage [31,32]. Moreover, the intracellular synthesis of GSH *in vivo* plays a critical role in the oocyte cytoplasm maturation, the formation and maintenance of meiotic spindles and the formation of embryonic pronuclei after fertilization [33,34]. Several studies have found that the limited capacity to synthesize GSH in bovine and porcine oocytes during IVM limited the gametogenic potential, which could be ameliorated by addition of exogenous

GSH to the IVM medium. Kim et al. identified the antioxidant effect of exogenous GSH added to the IVF system of bovine oocytes [35]. Furthermore, Zhou et al. found that exogenous supplementation with GSH reduced the meiotic failure of porcine oocytes by decreasing excessive ROS production, DNA damage accumulation and apoptotic incidence [36]. Li et al. further confirmed that exogenous GSH supplementation benefited bovine embryonic development by decreasing the ROS production [37]. However, the promising effect of exogenous supplementation with GSH on ovine IVM requires further investigation.

Therefore, we investigated whether supplementation of exogenous GSH facilitated the IVM of ovine oocytes via the inhibition of ROS production; in addition, the potential effects of exogenous GSH supplementation on the developmental competence of ovine oocytes, especially the histone methylation levels and fertilization capacities, were investigated to confirm the beneficial effect of GSH on ovine IVF and provide a further basis for the promising applications of GSH in the clinic.

## 2. Materials and methods

### 2.1. Ethics statement

All animal-related experimental protocols applied in this study were conducted under the standards of the Ethics Committee of Inner Mongolia University.

### 2.2. Chemicals

Unless otherwise indicated, all chemicals, supplements and culture medium used in this study were purchased from Sigma-Aldrich (Shanghai, China).

### 2.3. COCs collection

The ovine ovaries were collected from a local slaughterhouse in Hohhot, Inner Mongolia and transported within 2 h to the laboratory in prewarmed normal saline solution supplemented with 100 IU/mL penicillin and 100 IU/mL streptomycin solution (P/S, 15140122, Thermo Fisher, Shanghai, China) at 25–30 °C. Once the ovaries arrived, they were thoroughly rinsed with 70 % ethanol, followed by three washes with prewarmed normal saline solution, and the collection of cumulus oocyte complexes (COCs) was performed as described previously [38].

Briefly, the ovaries were placed in 35 mm sterile dishes (Corning, Beijing, China) containing dissecting medium [TCM-199 medium (11150067, Thermo Fisher, Shanghai, China) supplemented with 4 mg/mL bovine serum albumin (BSA, A3803, Sigma-Aldrich, Shanghai, China), 2 µg/mL heparin sodium (CH6021, Coolaber, Beijing, China), 1 mM HEPES (15630, Thermo Fisher, Shanghai, China) and 100 IU/mL penicillin/streptomycin]. The COCs were released from the ovaries with sterilized forceps and surgical blades and collected for the following IVM.

### 2.4. IVM

The COCs were divided into three grades based on the layer number of cumulus cells surrounding oocytes according to previously defined criteria [39]. Briefly, Grade A COCs had more than five layers of cumulus cells. Grade B COCs had approximately three to four layers of cumulus cells, while Grade C COCs had less than three layers of cumulus cells. Denuded oocytes and COCs with either general expansion of cumulus cells or discoloured cytoplasm of oocytes were excluded from the following study.

Furthermore, the conditions for COCs of each grade during IVM

were set established based on the addition of exogenous GSH to the maturation medium with the following experimental design: the negative control groups (NC group) for the three types of COCs were supplemented with Dulbecco's phosphate-buffered saline (DPBS) solution (14190250, Thermo Fisher, Shanghai, China), and the GSH groups of the three types of COCs were supplemented with 4 mM GSH (P1644, Sigma Aldrich, Shanghai, China). GSH was dissolved in DPBS solution and diluted in TCM-199 medium to a final concentration of 4 mM according to a previous study on GSH supplementation and porcine oocyte maturation [36].

These COCs were randomly assigned to the above experimental groups (repeated in triplicate), transferred to maturation medium drops (500  $\mu$ L for 40–50 COCs) covered by mineral oil (M8410, Sigma Aldrich, Shanghai, China) in a 4-well culture dish and cultured at 38.5 °C and 5 % CO<sub>2</sub> for 24 h. The basic maturation medium was TCM-199 medium supplemented with 10 % foetal bovine serum (FBS, 30044333, Thermo Fisher, Shanghai, China), 10 U/mL FSH (Ningbo Sansheng, Ningbo, China), 10 U/mL LH (Ningbo Sansheng, Ningbo, China), 2 mM GlutaMAX (35050061, Thermo Fisher, Shanghai, China), 100  $\mu$ M cysteamine (M9768, Sigma Aldrich, Shanghai, China), 0.3 mM sodium pyruvate (11360070, Thermo Fisher, Shanghai, China), 10 ng/mL EGF (31509, PEPRO TECH, Hangzhou, China) and 1  $\mu$ g/mL  $\beta$ -2-oestradiol (E8875, Sigma Aldrich, Shanghai, China) [40–42].

## 2.5. Oocyte maturation analyses and experimental design

After IVM, COCs of different groups were collected from the maturation medium, treated with fresh HEPES-synthetic oviductal fluid (H-SOF) medium supplemented with 400 IU/mL hyaluronidase (H3506, Sigma Aldrich, Shanghai, China) at 38 °C for 3 min and gently pipetted to remove cumulus cells. All denuded oocytes of different groups were collected, rinsed three times in fresh H-SOF medium and examined microscopically, followed by analysis of the maturation rate of MII oocytes in different groups (for the maturation rate analysis, n = 113 for the Grade A-NC group, n = 109 for the Grade B-NC group, n = 112 for the Grade C-NC group, n = 109 for Grade A-GSH group, n = 116 for the Grade B-GSH group and n = 116 for the Grade C-GSH group) [43].

After maturation rate analysis, MII oocytes were matured, collected and assigned to six groups for the following experiments according to the experimental group settings. Briefly, MII oocytes of the Grade A-NC group (n = 382), the Grade B-NC group (n = 374) and the Grade C-NC group (n = 385) were matured from the Grade A, Grade B and Grade C COCs of the NC groups, respectively, and MII oocytes of the Grade A-GSH group (n = 392), the Grade B-GSH group (n = 370) and the Grade C-GSH group (n = 365) were matured from the Grade A, Grade B and Grade C COCs of the GSH groups.

## 2.6. Immunofluorescence staining

MIII oocytes of each group were individually fixed in 4 % paraformaldehyde solution (PFA, P1110, Solarbio, Beijing, China) at room temperature for 30 min and permeabilized in 0.5 % Triton X-100 solution (T8200, Solarbio, Beijing, China) for 20 min at room temperature. Then, the oocytes were blocked with 1 % BSA solution (SW3015, Solarbio, Beijing, China) for 1 h, followed by incubation with primary antibodies at 4 °C overnight.

The primary antibodies used in this study were as follows: a fluorescein-labelled lens culinaris agglutinin antibody (LCA-FITC for cortical granules, as CGs, FL-1041, Vector Laboratories, CA, USA), a rabbit polyclonal anti-ASTL antibody (1:300, 204690-T08, Sino Biological, Beijing, China), a rabbit polyclonal anti-H3K4me3 antibody (1:300, ab136455, Absin, Beijing, China) and a rabbit

polyclonal anti-H3K9me3 antibody (1:300, EPR16601, Abcam, Shanghai, China).

After three washes (5 min for each time) with DPBS supplemented with 1 % Tween 20 (T8220, Solarbio, Beijing, China) and 0.01 % Triton-X 100, the oocytes immunostained with LCA-FITC were mounted on glass slides. In addition, the oocytes incubated with ASTL, H3K4me3 and H3K9me3 antibodies were individually incubated with the corresponding secondary antibody for 1 h at room temperature. The secondary antibodies used in this study were as follows: an Alexa Fluor® 647 secondary antibody (1:300, ab150075, Abcam, Shanghai, China) for H3K9me3 and an Alexa Fluor® 555 secondary antibody (1:300, ab150074, Abcam, Shanghai, China) for ASTL and H3K4me3.

After three washes (5 min for each time) with DPBS, the oocytes immunostained with ASTL were collected and mounted on glass slides. Furthermore, the oocytes immunostained with H3K4me3 and H3K9me3 antibodies were incubated with 5  $\mu$ g/mL Hoechst 33342 solution (B8040, Solarbio, Beijing, China) for 10 min at room temperature, followed by oocyte mounting.

All oocytes were examined under a confocal microscope (A1R, Nikon, Tokyo, Japan) after immunofluorescence staining, and the relative fluorescence intensity of each group (n = 30 for each group) was analysed by ImageJ software.

## 2.7. Mitochondrial activities analyses of MII oocytes

MIII oocytes of different groups were randomly collected, subsequently stained with 200 nM fresh MitoTracker Red CMXRos solution (C1049, Beyotime, Haimen, China) for 30 min at 37 °C. After staining and examination under a confocal microscope, the fluorescence staining densities of MitoTracker in the MII oocytes were calculated with ImageJ software to analyse the mitochondrial activities of different groups (n = 30 for each group).

## 2.8. Analyses of ROS production of MII oocytes

MIII oocytes of different groups (n = 30 for each group) were randomly collected and incubated in H-SOF medium containing 10  $\mu$ M dichlorofluorescein diacetate (DCFH-DA, S0033, Beyotime, Haimen, China) for 30 min at 37 °C according to the manufacturer's protocols [44]. After incubation of DCFH-DA and oocyte mounting on glass slides, DCFH-DA staining of MII oocytes was assessed under a confocal microscope. The fluorescence staining densities of MII oocytes were calculated with ImageJ software to analyse the relative ROS levels of different groups.

## 2.9. RNA extraction and quantitative real-time PCR (qRT-PCR)

Denuded MII oocytes of different groups (n = 30 for each group) were randomly collected, followed by the RNA extraction with an RNeasy Mini Kit (74134, Qiagen, Beijing, China). The reverse transcription of cDNA was carried out by a commercial Prime Script™ RT reagent kit (RR047A, Takara, Dalian, China), followed by the real-time PCR performed by SYBR PremixEx Taq (RR820A, Takara, Dalian, China) with a Thermo Scientific Pikoreal machine. The relative gene expression levels were calculated by the 2<sup>- $\Delta\Delta$ Ct</sup> method with  $\beta$ -actin (ubiquitously expressed gene) applied as an internal control [45]. All PCR experiments were performed in triplicate to confirm the data. The gene primers applied in this study are shown in Supplement Table 1.

## 2.10. IVF

Before IVF, the MII oocytes of different groups were individually transferred into the fertilization medium as 500  $\mu$ L drops of SOF

**Table 1**  
The effect of exogenous GSH supplementation on the gene expression levels of ovine MII oocytes.

Group Gene	Grade A		Grade B		Grade C	
	NC	GSH	NC	GSH	NC	GSH
<i>Gdf9</i>	1.00	1.42 ± 0.09*	1.00	2.42 ± 0.04*	1.00	3.22 ± 0.12*
<i>Bmp15</i>	1.00	1.25 ± 0.08*	1.00	2.33 ± 0.03*	1.00	2.74 ± 0.14*
<i>Oct4</i>	1.00	1.63 ± 0.17*	1.00	2.59 ± 0.04*	1.00	2.91 ± 0.08*
<i>Gpx</i>	1.00	1.67 ± 0.12*	1.00	2.85 ± 0.05*	1.00	3.36 ± 0.05*
<i>Sod2</i>	1.00	1.79 ± 0.15*	1.00	2.30 ± 0.08*	1.00	2.62 ± 0.03*
<i>Catalase</i>	1.00	1.65 ± 0.10*	1.00	2.04 ± 0.10*	1.00	2.90 ± 0.16*
<i>Bcl2</i>	1.00	1.30 ± 0.13*	1.00	1.49 ± 0.04*	1.00	1.85 ± 0.08*
<i>Bax</i>	1.00	0.80 ± 0.07*	1.00	0.72 ± 0.05*	1.00	0.72 ± 0.03*
<i>Caspase3</i>	1.00	0.68 ± 0.05*	1.00	0.81 ± 0.05*	1.00	0.72 ± 0.04*
<i>Kdm5b</i>	1.00	1.31 ± 0.07*	1.00	1.90 ± 0.03*	1.00	2.28 ± 0.04*
<i>Kdm4d</i>	1.00	1.38 ± 0.04*	1.00	2.22 ± 0.11*	1.00	2.90 ± 0.10*

Note: NC represents the negative control groups, and GSH represents the exogenous GSH supplementation groups. The experimental data were analysed by a one-way ANOVA with post-hoc comparisons and  $p < 0.05$  was accepted as significant. \* in each column indicates significant differences between the GSH group and the corresponding NC group.

medium supplemented with 2 % oestrus ovine serum, 2 mM sodium pyruvate, 10 µg/mL heparin sodium and 1 mM caffeine (58082, Amresco, Shanghai, China) in a 4-well culture dish and cultured in a CO<sub>2</sub> incubator (38.5 °C, 5 % O<sub>2</sub> and 5 % CO<sub>2</sub>).

For IVF, frozen semen straws purchased from a local company (LEKE) were removed from the liquid nitrogen, kept in air for 10 s and thawed in a water bath at 38 °C for 15 s. After centrifugation with 90 % Percoll and 45 % Percoll solution (P1644, Sigma-Aldrich, Shanghai, China) diluted with the fertilization medium at 2100 rpm for 15 min, the spermatozoa were carefully collected from the bottom of a centrifuge tube, and the number of spermatozoa was counted.

After sperm number counting, the spermatozoa at a final concentration of approximately  $1 \times 10^6$  sperm/mL were transferred to the above fertilization medium containing MII oocytes and cultured for 18 h in a CO<sub>2</sub> incubator (38.5 °C, 5 % O<sub>2</sub> and 5 % CO<sub>2</sub>).

### 2.11. Sperm binding assay

During IVF, the number of sperm binding to the MII oocytes of different groups was determined [46–48]. Briefly, after fertilization for 1 h, the MII oocytes of different groups were randomly collected, fixed in 4 % PFA at room temperature for 30 min and stained with 10 µg/mL Hoechst 33342 solution in the dark for 10 min. The sperm binding to the MII oocytes of different groups were analysed and quantified under a confocal microscope (n = 30 for each group).

### 2.12. Assessment of fertilization

After fertilization, the embryos of different groups (n = 142 for the Grade A-NC group, n = 152 for the Grade A-GSH group, n = 134 for the Grade B-NC group, n = 130 for the Grade B-GSH group, n = 145 for the Grade C-NC group and n = 125 for the Grade C-GSH group) were individually transferred to SOF medium supplemented with 4 mg/mL BSA, 2 % essential amino acids (11130051, Thermo Fisher, Shanghai, China), 1 % nonessential amino acids (M7145, Sigma Aldrich, Shanghai, China), 2 mM GlutaMAX, 1 mM sodium pyruvate, 2.8 mM myo-inositol (18050, Solarbio, Beijing, China) and 0.5 mM sodium citrate (T7461, Solarbio, Beijing, China) covered by mineral oil in a 35 mm sterile dish, followed by subsequent embryos culture in a CO<sub>2</sub> incubator (38.5 °C, 5 % O<sub>2</sub> and 5 % CO<sub>2</sub>).

After 48 h, the presence of embryo cleavage in the fertilized embryos in different groups, as the successful symbol of fertilization, was examined under a stereomicroscope (745T, Nikon, Tokyo,

China). The embryos of different groups were cultured *in vitro* for the following 7 d with the culture medium changed every 48 h.

During the embryo culture process, the developmental rates of 2-cell embryos and blastocysts in different groups were microscopically observed and analysed, and the embryonic development rates were calculated as the percentage of surviving embryos/fertilized MII oocytes.

### 2.13. Statistical analyses

The analyses of the experimental results in this study were conducted with the Statistical Package for the Social Sciences software (SPSS, IBM, Version 19.0) and Microsoft Excel. All experimental data, presented as mean ± SD, were tested with a General Linear Model (GLM) prior to the following statistical analyses of different groups. And the experimental data including maturation rates, relative fluorescence intensities (CGs, ASTL, MitoTracker, DCHE-DA, H3K4me3 and H3K9me3), gene expression levels, blastocyst development rates and cell number/blastocyst among different groups were assessed by a one-way ANOVA with post-hoc comparisons.  $p < 0.05$  was defined as significant in the present study.

## 3. Results

### 3.1. The effect of exogenous GSH supplementation on the maturation rates of ovine oocytes

First, the effects of exogenous GSH supplementation on the maturation rates of ovine oocytes were determined by assessing the occurrence rates of polar body extrusion (PBE) in different groups, and the results are shown in Fig. 1.

We found that exogenous GSH supplementation significantly enhanced the oocyte maturation rates of the Grade B and Grade C groups ( $p < 0.05$ ), with the maturation rates of the Grade B group significantly increasing from  $75.15 \pm 3.29$  % (n = 109, Grade B-NC group) to  $82.83 \pm 1.69$  % (n = 116, Grade B-GSH group) and that of the Grade C group significantly increasing from  $70.78 \pm 2.34$  % (n = 112, Grade C-NC group) to  $77.66 \pm 0.99$  % (n = 116, Grade C-GSH group). Moreover, GSH had no significant effect on the oocyte maturation rates of the Grade A groups; the maturation rates were  $88.70 \pm 2.57$  % for the Grade A-NC group (n = 113) and  $86.81 \pm 3.66$  % for the Grade A-GSH group (n = 109,  $p > 0.05$ ).

### 3.2. The effect of exogenous GSH supplementation on the cytoplasmic maturation levels of ovine MII oocytes

Due to the important roles of CGs in the cytoplasmic maturation process of mammalian oocytes and the prevention of polyspermy after fertilization, the dynamics of CGs in ovine MII oocytes of different groups were analysed by LCA-FITC staining, and representative images are presented in Fig. 2.

As shown in Fig. 2, the results of the CGs dynamics in the ovine MII oocytes of different groups showed that the CGs signals (mainly detected in the subcortical region of MII oocytes) of the NC groups were significantly reduced with the decreasing number of cumulus layers (n = 30 for each NC group). Furthermore, exogenous GSH supplementation significantly enhanced the fluorescence intensity of CGs signals of the GSH groups compared with those of the corresponding NC groups, regardless of the number of cumulus layers (n = 30 for each GSH group,  $p < 0.05$ , Fig. 2 I,II).

Moreover, the expression patterns of ASTL in the ovine MII oocytes of different groups were analysed, and the representative images are presented in Fig. 2III.

As shown in Fig. 2III, the results of ASTL staining of the NC

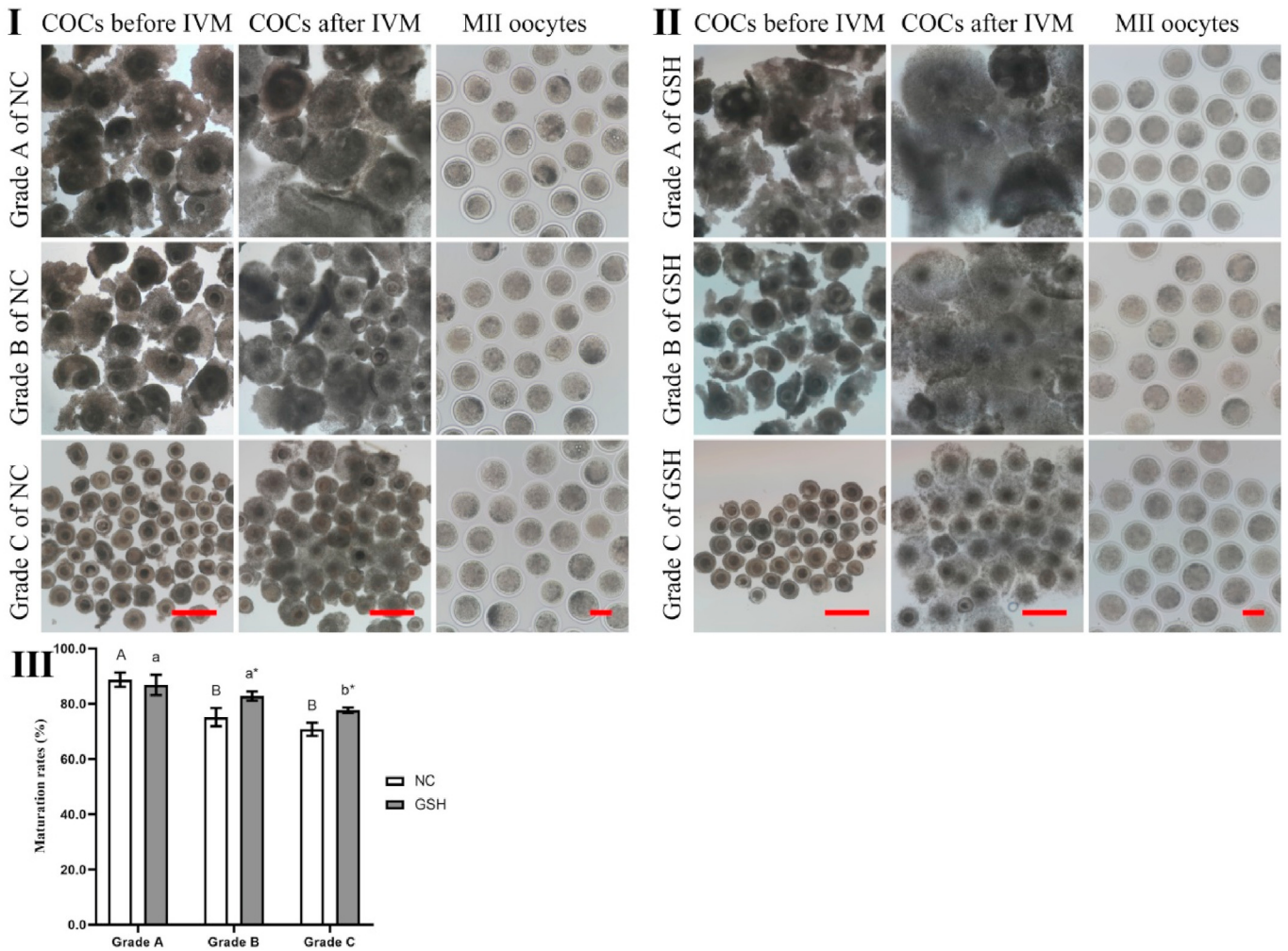


**Fig. 1.** The effect of exogenous GSH supplementation on the IVM rates of ovine COCs I: Morphology of COCs before IVM, COCs after IVM and MII oocytes of NC groups. Note: The scale bar of COCs before IVM = 500 μm. The scale bar of COCs after IVM = 500 μm. The scale bar of MII oocytes = 100 μm. II: Morphology of COCs before IVM, COCs after IVM and MII oocytes of GSH group. Note: The scale bar of COCs before IVM = 500 μm. The scale bar of COCs after IVM = 500 μm. The scale bar of MII oocytes = 100 μm. III: The maturation rates. Note: NC represents the negative control groups and GSH represents the exogenous GSH supplementation groups. The experimental data were analysed by a one-way ANOVA with post-hoc comparisons and  $p < 0.05$  was accepted as significant. The different uppercase letters in each column indicate significant differences between the NC groups. The different lowercase letters in each column indicates significant differences between the GSH groups. \* in each column indicates significant differences between the GSH group and the corresponding NC group.

groups were consistent with the results of CGs dynamics of the NC groups, as the ASTL signals of the NC groups were significantly reduced in a dose-dependent manner with the decrease in cumulus layers ( $n = 30$  for each NC group,  $p < 0.05$ ). In addition, ASTL staining further revealed that exogenous GSH supplementation significantly enhanced the staining intensity of ASTL compared with that of the corresponding NC groups ( $n = 30$  for each GSH group,  $p < 0.05$ , Fig. 2 III, IV), regardless of the number of cumulus layers, indicating that exogenous GSH supplementation during IVM promoted the cytoplasmic maturation levels of ovine MII oocytes.

### 3.3. The effect of exogenous GSH supplementation on the mitochondrial activities of ovine MII oocytes

To investigate the effect of exogenous GSH supplementation on the developmental competence of ovine MII oocytes, we analysed the mitochondrial activities in the ovine MII oocytes of different groups, and representative MitoTracker staining results are presented in Fig. 3.

As shown in Fig. 3, the fluorescence staining results of MitoTracker Red CMXRos of the NC group revealed the key role of cumulus cells in the developmental competence of ovine oocytes during IVM, as the fluorescence intensities of MitoTracker in the NC groups were significantly reduced from the Grade A-NC group and the Grade B-NC group to the Grade C-NC group ( $n = 30$  for each NC group,  $p < 0.05$ ).

In addition, the MitoTracker staining intensities of the Grade B-GSH and Grade C-GSH groups were strongly enhanced compared with those of the corresponding NC groups ( $n = 30$  for each GSH group,  $p < 0.05$ ). There was no significant difference in the MitoTracker staining intensities between the Grade A-NC and Grade A-GSH groups ( $p > 0.05$ ), further indicating that exogenous GSH supplementation during IVM promoted the developmental competence of ovine MII oocytes, especially for MII oocytes matured from COCs lacking cumulus cells.

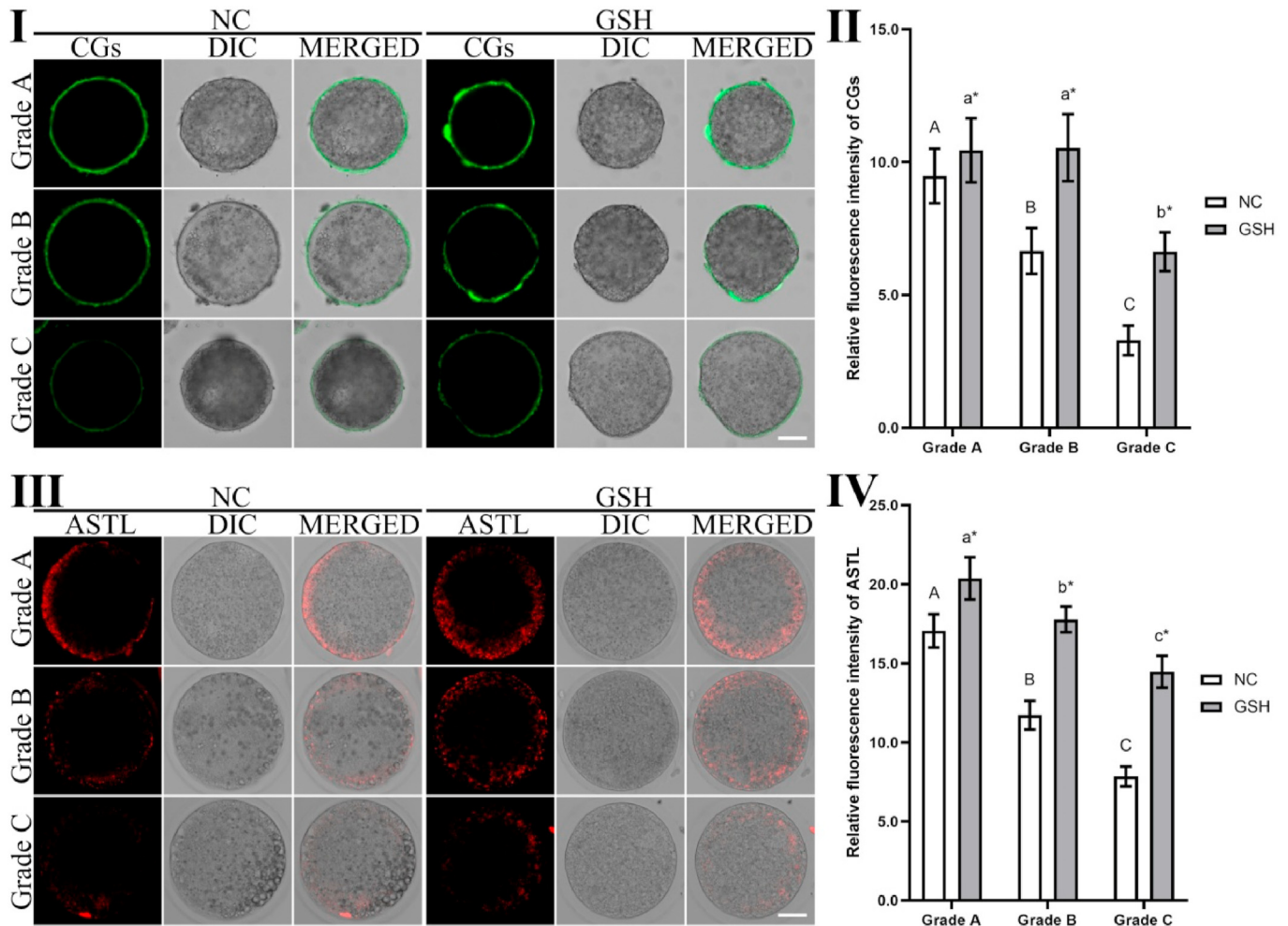


**Fig. 2.** The effect of exogenous GSH supplementation on the cytoplasmic maturation levels of ovine MII oocytes I: CGs dynamics. Note: NC represents the negative control groups, and GSH represents the exogenous GSH supplementation groups. CGs represents LCA-FITC staining specific for the CGs dynamics of ovine MII oocytes. DIC, differential interference contrast microscope, represents the bright field view of ovine MII oocytes after LCA-FITC staining. MERGED represents the merged result of LCA-FITC staining and bright field microscopy. The scale bar = 50  $\mu$ m. II: The relative fluorescence intensity of CGs. Note: NC represents the negative control groups and GSH represents the exogenous GSH supplementation groups. The experimental data were analysed by a one-way ANOVA with post-hoc comparisons and  $p < 0.05$  was accepted as significant. The different uppercase letters in each column indicate significant differences between the NC groups. The different lowercase letters in each column indicates significant differences between the GSH groups. \* in each column indicates significant differences between the GSH group and the corresponding NC group. III: **ASTL stainings.** Note: NC represents the negative control groups, and GSH represents the exogenous GSH supplementation groups. ASTL represents ASTL staining. DIC represents the bright field view of ovine MII oocytes after ASTL staining. MERGED represents the merged result of ASTL staining and bright field microscopy. The scale bar = 50  $\mu$ m IV: The relative fluorescence intensity of ASTL. Note: NC represents the negative control groups and GSH represents the exogenous GSH supplementation groups. The experimental data were analysed by a one-way ANOVA with post-hoc comparisons and  $p < 0.05$  was accepted as significant. The different uppercase letters in each column indicate significant differences between the NC groups. The different lowercase letters in each column indicates significant differences between the GSH groups. \* in each column indicates significant differences between the GSH group and the corresponding NC group.

**3.4. The effect of exogenous GSH supplementation on the ROS production of ovine MII oocytes**

To investigate the effect of exogenous GSH supplementation on the ROS production of ovine MII oocytes, we measured the ROS levels in the MII oocytes of different groups by DCFH-DA fluorescence staining, with the representative results shown in Fig. 4.

The increasing staining intensities of DCFH-DA from the Grade A-NC group and Grade B-NC group to the Grade C-NC group further indicated that the ROS levels in the ovine MII oocytes during IVM were negatively related to the number of cumulus layers ( $n = 30$  for each NC group,  $p < 0.05$ ), confirming the key role of cumulus cells in the developmental competence of ovine MII oocytes during IVM.

In contrast, the staining intensities of DCFH-DA in all GSH groups were effectively reduced compared with those of the

corresponding NC groups ( $n = 30$  for each GSH group,  $p < 0.05$ ), further indicating the antioxidant effect of exogenous GSH supplementation on the developmental competence of ovine MII oocytes.

**3.5. The effect of exogenous GSH supplementation on the gene expression levels of ovine MII oocytes**

To assess the effect of exogenous GSH supplementation on the gene expression patterns of ovine MII oocytes, we analysed the expression levels of specific genes related to oocyte maturation (*Oct4*, *Bmp15* and *GDF9*), antioxidative effects (*SOD2*, *Catalase* and *Gpx*), apoptotic processes (*BAX* and *Bcl-2*) and histone methylation (*Kdm4d* and *Kdm5b*) in ovine MII oocytes by qRT-PCR.

As shown in Table 1, the relative expression levels of specific

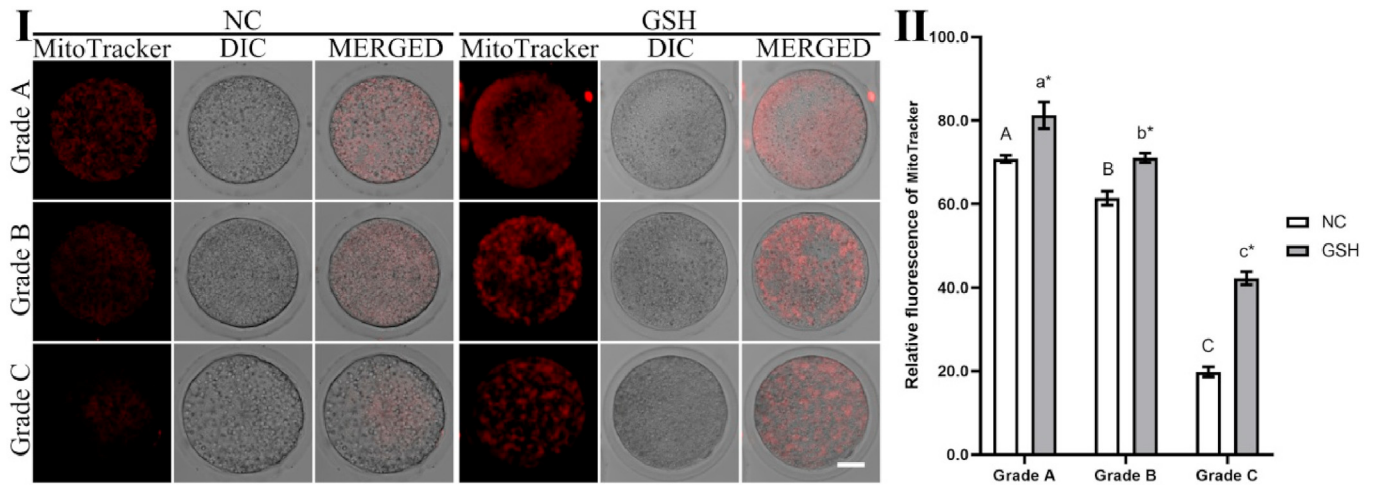


**Fig. 3.** The effect of exogenous GSH supplementation on the mitochondrial activities of ovine MII oocytes I: MitoTracker Red CMXRos stainings. Note: NC represents the negative control groups, and GSH represents the exogenous GSH supplementation groups. MitoTracker represents the MitoTracker Red CMXRos staining of different groups. DIC represents the bright field view of ovine MII oocytes after MitoTracker Red CMXRos staining. MERGED represents the merged result of MitoTracker Red CMXRos staining and bright field microscopy. The scale bar = 50  $\mu$ m. II: The relative fluorescence intensity of MitoTracker. Note: NC represents the negative control groups and GSH represents the exogenous GSH supplementation groups. The experimental data were analysed by a one-way ANOVA with post-hoc comparisons and  $p < 0.05$  was accepted as significant. The different uppercase letters in each column indicate significant differences between the NC groups. The different lowercase letters in each column indicates significant differences between the GSH groups. \* in each column indicates significant differences between the GSH group and the corresponding NC group.

genes related to oocyte maturation (*Oct4*, *Bmp15* and *GDF9*), anti-oxidative effects (*SOD2*, *Catalase* and *GPx*) and antiapoptotic effects (*Bcl-2*) in all GSH groups were significantly up-regulated compared with those of the corresponding NC groups ( $n = 30$  for each group,  $p < 0.05$ ). In contrast, the relative gene expression levels of *Bax* in the GSH groups were significantly lower than those in the corresponding NC groups ( $p < 0.05$ ).

Furthermore, the expression levels of *Kdm4d* and *Kdm5b* in all GSH groups were significantly enhanced compared with those of the corresponding NC groups ( $p < 0.05$ ), which further indicates that exogenous GSH supplementation promoted the histone methylation levels of ovine MII oocytes.

### 3.6. The effect of exogenous GSH supplementation on the methylation levels of ovine MII oocytes

To further confirm the effect of exogenous GSH supplementation on the histone methylation levels of ovine MII oocytes, we determined the expression levels of H3K4me3 and H3K9me3 in the MII oocytes of different groups ( $n = 30$  for each group) by immunofluorescence staining, with representative results shown in Fig. 5.

As shown in Fig. 5, the H3K4me3 expression levels of the NC groups were significantly reduced from the Grade A-NC group and the Grade B-NC group to the Grade C-NC group ( $p < 0.05$ ), which

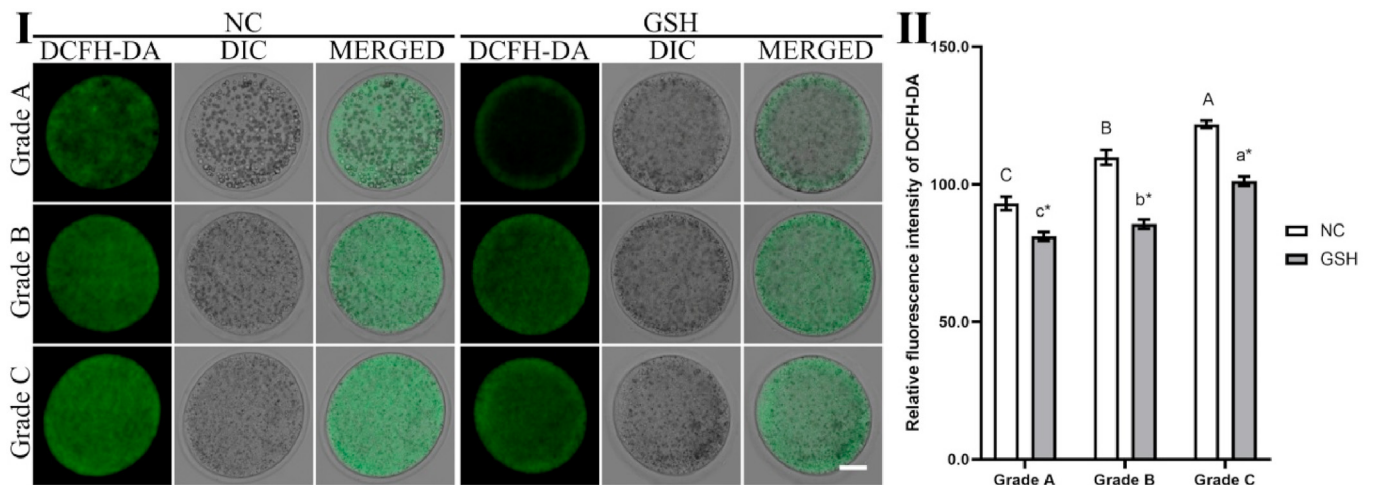


**Fig. 4.** The effect of exogenous GSH supplementation on the ROS production levels of ovine MII oocytes I: DCFH-DA staining. Note: NC represents the negative control groups, and GSH represents the exogenous GSH supplementation groups. DCFH-DA represents the DCFH-DA staining of different groups. DIC represents the bright field view of ovine MII oocytes after DCFH-DA staining. MERGED represents the merged result of DCFH-DA staining and bright field microscopy. The scale bar = 50  $\mu$ m. II: The relative fluorescence intensity of DCFH-DA. Note: NC represents the negative control groups and GSH represents the exogenous GSH supplementation groups. The experimental data were analysed by a one-way ANOVA with post-hoc comparisons and  $p < 0.05$  was accepted as significant. The different uppercase letters in each column indicate significant differences between the NC groups. The different lowercase letters in each column indicates significant differences between the GSH groups. \* in each column indicates significant differences between the GSH group and the corresponding NC group.

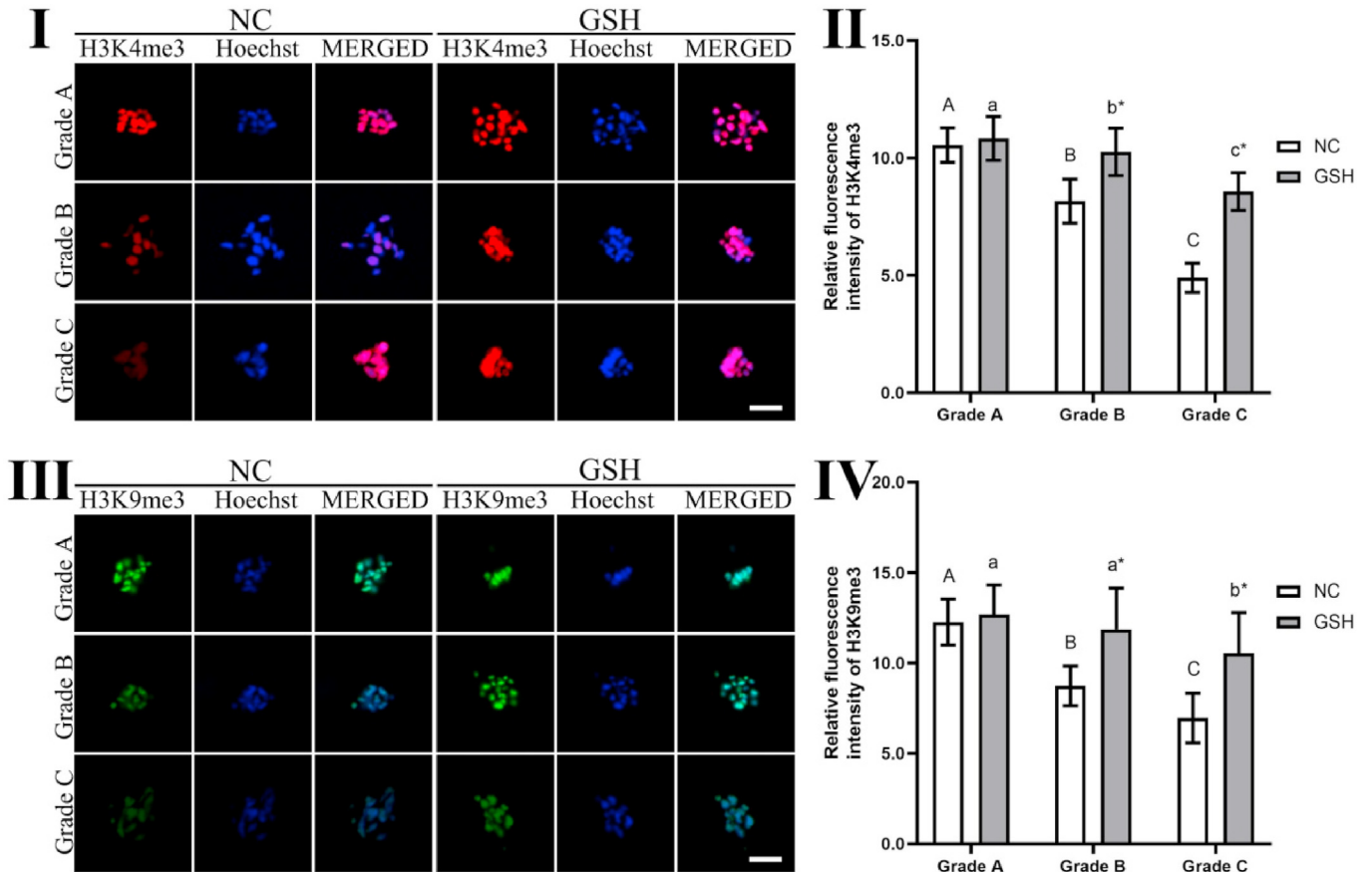


**Fig. 5.** The effect of exogenous GSH supplementation on the histone methylation levels of ovine MII oocytes I: Immunofluorescence staining of H3K4me3. Note: NC represents the negative control groups, and GSH represents the exogenous GSH supplementation groups. H3K4me3 represents the immunofluorescence staining of H3K4me3 of different groups. Hoechst represents the Hoechst33342 staining of different groups after H3K4me3 staining. MERGED represents the merged result of H3K4me3 staining and Hoechst33342 staining. The scale bar = 5 μm. II: The relative fluorescence intensity of H3K4me3. Note: NC represents the negative control groups and GSH represents the exogenous GSH supplementation groups. The experimental data were analysed by a one-way ANOVA with post-hoc comparisons and  $p < 0.05$  was accepted as significant. The different uppercase letters in each column indicate significant differences between the NC groups. The different lowercase letters in each column indicates significant differences between the GSH groups. \* in each column indicates significant differences between the GSH group and the corresponding NC group. III: Immunofluorescence staining of H3K9me3. Note: NC represents the negative control groups, and GSH represents the exogenous GSH supplementation groups. H3K9me3 represents the immunofluorescence staining of H3K9me3 of different groups. Hoechst represents the Hoechst33342 staining of different groups after H3K9me3 staining. MERGED represents the merged result of H3K9me3 staining and Hoechst33342 staining. The scale bar = 5 μm IV: The relative fluorescence intensity of H3K9me3. Note: NC represents the negative control groups and GSH represents the exogenous GSH supplementation groups. The experimental data were analysed by a one-way ANOVA with post-hoc comparisons and  $p < 0.05$  was accepted as significant. The different uppercase letters in each column indicate significant differences between the NC groups. The different lowercase letters in each column indicates significant differences between the GSH groups. \* in each column indicates significant differences between the GSH group and the corresponding NC group.

further revealed that the expression of H3K4me3 in ovine MII oocytes was negatively related to a decrease in the cumulus layers. In addition, the expression levels of H3K4me3 in the GSH groups were enhanced compared with those in the corresponding NC groups, especially in MII oocytes of the Grade B-GSH and Grade C-GSH groups ( $p < 0.05$ , Fig. 5 I, II).

Moreover, the H3K9me3 expression levels of the NC groups were abnormally reduced from the Grade A-NC group and the Grade B-NC group to the Grade C-NC group ( $p < 0.05$ , Fig. 5 III,IV). Conversely, the abnormal expression levels of H3K9me3 in ovine MII oocytes were effectively enhanced by exogenous GSH supplementation ( $p < 0.05$ , Fig. 5 III, IV).

Combined with the qRT-PCR results, these above results further indicated that exogenous GSH supplementation ameliorated the abnormal modifications of histone methylation in ovine MII oocytes.

### 3.7. The effect of exogenous GSH supplementation on the sperm binding and fertilization abilities of ovine MII oocytes

To confirm the beneficial effect of exogenous GSH supplementation on the *in vitro* developmental competence of ovine MII oocytes, we performed a sperm-oocyte binding assay after IVF, followed by Hoechst 33342 staining and determination of the number of sperm binding to the zona pellucida of ovine MII oocytes ( $n = 30$  for each group).

As shown in Supplementary Fig. 1, the number of sperm binding to the zona pellucida of the NC groups was substantially reduced from the Grade A-NC group ( $199.93 \pm 16.50$ ) to the Grade B-NC group ( $161.967 \pm 11.75$ ) and the Grade C-NC ( $106.63 \pm 6.98$ ) group ( $p < 0.05$ ), indicating the decreasing qualities of ovine MII oocytes due to the lack of cumulus layers during IVM. The number of sperm binding to the zona pellucida of the GSH groups was effectively



increased from the Grade C-GSH group ( $166.20 \pm 11.26$ ) to the Grade B-GSH group ( $193.07 \pm 14.42$ ) and the Grade A-GSH ( $250.97 \pm 26.00$ ) group ( $p < 0.05$ ), while the number of sperm binding to the zona pellucida of the GSH groups was significantly enhanced compared with that of the corresponding NC groups ( $p < 0.05$ ).

Furthermore, the results of embryonic cleavage assays indicated that exogenous GSH supplementation significantly enhanced the fertilization rates of the Grade B-GSH and Grade C-GSH groups ( $p < 0.05$ ), with the fertilization rates of the Grade B groups significantly increasing from  $70.73 \pm 2.85\%$  ( $n = 134$ , Grade B-NC group) to  $79.93 \pm 4.72\%$  ( $n = 130$ , Grade B-GSH group) and that of the Grade C groups significantly increasing from  $58.15 \pm 4.30\%$  ( $n = 145$ , Grade C-NC group) to  $71.24 \pm 4.34\%$  ( $n = 125$ , Grade C-GSH group). In addition, there was no significant difference in the fertilization rates between the Grade A-NC ( $n = 142$ ,  $79.81 \pm 3.13\%$ ) and Grade A-GSH ( $n = 152$ ,  $83.50 \pm 4.56\%$ ) groups ( $p > 0.05$ ).

### 3.8. The effect of exogenous GSH supplementation on the blastocyst developmental competence of ovine MII oocytes

Blastocyst development experiments were performed to confirm the effect of exogenous GSH supplementation on the *in vitro* developmental competence of ovine MII oocytes, and the results are presented in Fig. 6.

As shown in Fig. 6, the blastocyst developmental rates of different groups indicated that exogenous GSH supplementation promoted the blastocyst developmental rates compared with these of the NC groups; the blastocyst developmental rates of the Grade A groups increased from  $39.63 \pm 3.72\%$  ( $n = 113$ , Grade A-NC group) to  $40.92 \pm 3.11\%$  ( $n = 127$ , Grade A-GSH group) ( $p > 0.05$ ), that of the Grade B groups significantly increased from  $30.25 \pm 2.22\%$  ( $n = 95$ , Grade B-NC group) to  $40.68 \pm 2.39\%$  ( $n = 96$ , Grade B-GSH group) ( $p < 0.05$ ) and that of the Grade C groups significantly increased from  $18.01 \pm 2.77\%$  ( $n = 84$ , Grade C-NC group) to  $32.02 \pm 2.08\%$  ( $n = 87$ , Grade C-GSH group) ( $p < 0.05$ ).

Finally, Hoechst 33342 staining was performed to analyse the cell number/each blastocyst of different groups, and the results showed that exogenous GSH supplementation significantly enhanced the blastocyst qualities compared with those of the corresponding NC groups, with the cell number/each blastocyst of the Grade A groups significantly increasing from  $114.50 \pm 20.85$  ( $n = 30$ , Grade A-NC group) to  $143.37 \pm 28.17$  ( $n = 30$ , Grade A-GSH group), that of the Grade B group significantly increasing from  $93.33 \pm 17.01$  ( $n = 27$ , Grade B-NC group) to  $112.70 \pm 24.65$  ( $n = 30$ , Grade B-GSH group) and that of the Grade C group significantly increasing from  $76.07 \pm 13.68$  ( $n = 15$ , Grade C-NC group) to  $97.70 \pm 16.74$  ( $n = 27$ , Grade C-GSH group) ( $p < 0.05$ ).

## 4. Discussion

In this study, we found that exogenous GSH supplementation promoted the developmental competence of ovine MII oocytes via the effective promotion of nuclear/cytoplasmic maturation, CGs dynamics/ASTL distributions and mitochondrial activities. In addition, exogenous GSH supplementation effectively promoted the suppression of ROS production in ovine MII oocytes. Enhancement of the sperm binding abilities and fertilization capacity of ovine MII oocytes after exogenous GSH supplementation was also found in this study. We also found that exogenous GSH supplementation especially enhanced the *in vitro* developmental competence of ovine MII oocytes from COCs lacking cumulus cells, which revealed the potential applications of exogenous GSH supplementation for the IVM of patients with follicular dysplasia.

In the present study, the beneficial effect of exogenous GSH

supplementation on the nuclear and cytoplasmic maturation of ovine MII oocytes, confirmed by the results of CGs dynamics/ASTL distributions, was consistent with the former studies about bovine [37] and porcine oocytes [46]. In 1997, Misa et al. found that the CGs dynamics in bovine MII oocytes, significantly related with the cumulus cell layers in bovine COCs, closely parallels the maturation rates and fertilization potentials of bovine oocytes after IVM and could be applied as an index of cytoplasmic maturation of mammalian oocytes and embryonic development [49]. Combined with the correlations between CGs dynamics and oocyte maturation and the observation of absent CGs in mouse oocytes from the arrested follicles lacking surrounding cumulus granulosa cells [50], CGs dynamics were applied as the symbol of cytoplasmic maturation of ovine MII oocytes in this study and our results of LCA-FITC staining further confirmed the significant correlations between CGs dynamics in ovine MII oocytes and cumulus cell layers during IVM and the promising effect of exogenous GSH supplementation on ovine IVM.

In addition, we also found the exogenous GSH supplementation effectively enhanced the expression signals of ASTL in ovine MII oocytes. ASTL (also referred as ovastacin and sperm acrosomal SLLP1 binding protein), a key component of CGs in mammals, was identified as an oolemmal binding partner for the intra-acrosomal sperm protein SLLP1 and an oocyte-specific metalloendoprotease cleaving zona pellucida glycoprotein 2 (ZP2) ( $^{166}\text{LA}^1\text{DE}^{169}$ ) after fertilization [51,52]. Moreover, lacking of ASTL caused abnormal sperm binding as well to two-cell embryos as they did to the matured oocytes, causing polyspermy [53]. Considering the negative relationship between ASTL distributions and ROS related oxidative stress in mammalian oocytes [52], these former studies have found that the promising effect of antioxidants supplementation [51,52,54] on the mammalian IVM process via the promotion of ASTL distributions.

And the effect of exogenous GSH supplementation on the reduction of ROS accumulation related oxidative disturbance was also analysed by the mitochondrial activities and ROS production assay. The comprehensive results of MitoTracker staining, DCFH-DA staining and expression levels of genes including *Gpx*, *Sod2*, *Catalase*, *Bcl-2*, *Bax* and *Caspase 3* showed that exogenous GSH supplementation during ovine IVM process effectively enhanced the mitochondrial activities and decreased the ROS production levels, further enhancing the qualities of ovine MII oocytes and the subsequent fertilization and embryonic development.

In fact, the main differences between our study and previous studies examining the effect of exogenous GSH supplementation were the analyses of histone methylation levels of ovine MII oocytes, especially MII oocytes matured from COCs lacking cumulus cells.

As an important post-translational modification, histone methylation on the side chains of arginine and lysine in H2A, H2B, H3 and H4 regulates embryonic genome activation, X-chromosome inactivation (Xist) activation, inner cell mass (ICM)/trophoblast (TE) lineage specification and preimplantation development [55,56]. Furthermore, Yu et al. found that supplementation with L-ascorbic acid, as an epigenetic factor inducing global epigenetic reprogramming during IVM effectively improved the developmental competence of porcine oocytes via the reprogramming of DNA, RNA and histone methylation status [57]. Bui et al. also found that the increasing methylation levels of H3K4 via the supplementation of L-ascorbic acid during the pre-IVM process enhanced the developmental competence and quality of porcine blastocysts derived from small antral follicles [58], revealing the promising applications of antioxidants with the potential for histone methylation modifications in the IVM of mammalian COCs lacking cumulus cells.

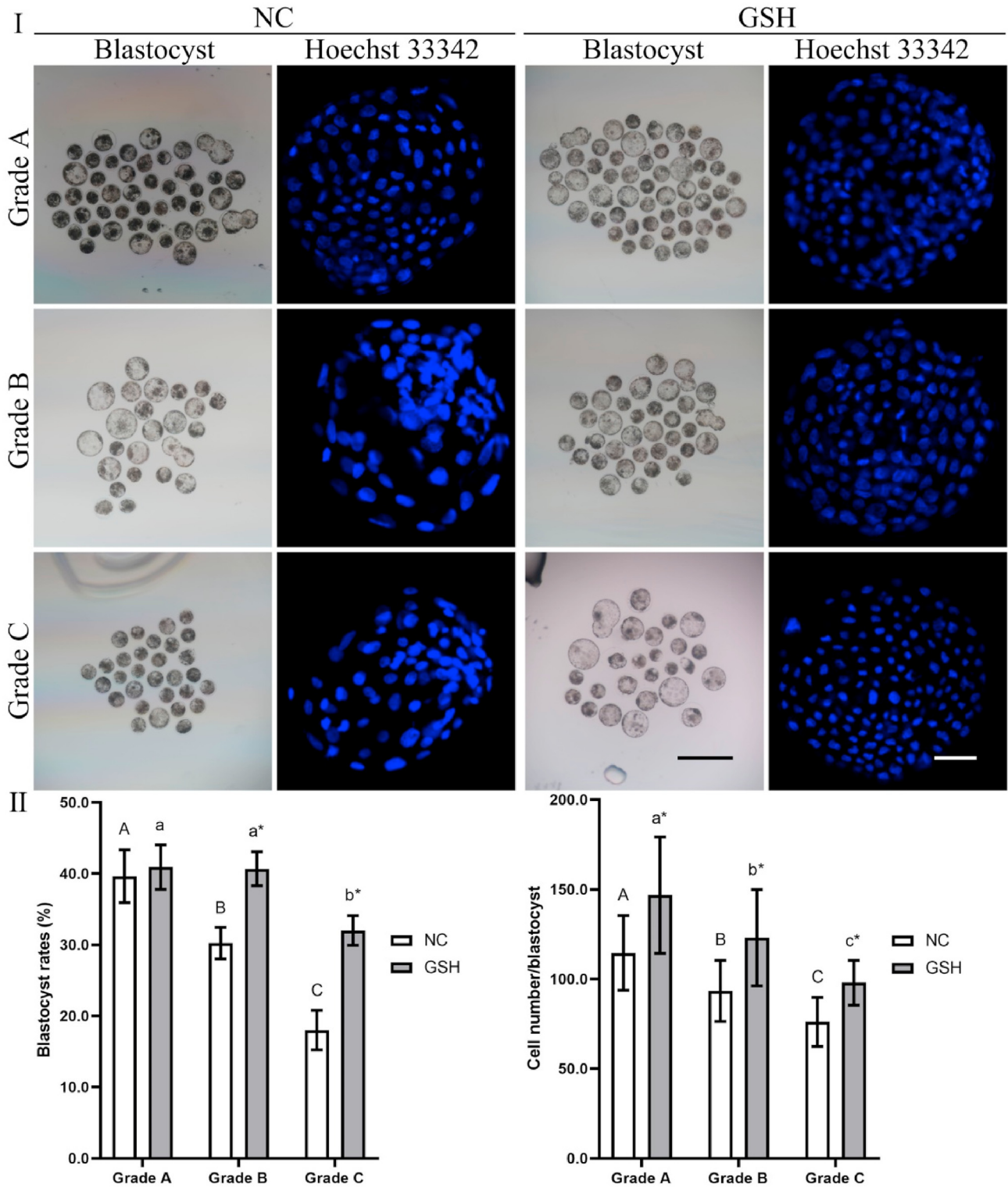


**Fig. 6.** The effect of exogenous GSH supplementation on the blastocyst developmental competence of ovine MII oocytes  
 I: The development and Hoechst 33342 staining of blastocysts. Note: NC represents the negative control groups, and GSH represents the exogenous GSH supplementation groups. Blastocyst represents the bright field view of blastocyst after IVF. Hoechst 33342 represents the Hoechst 33342 staining of blastocysts. The scale bar of blastocyst = 500 μm. The scale bar of Hoechst 33342 staining = 50 μm. II: The blastocyst rates and cell number/blastocyst. Note: NC represents the negative control groups and GSH represents the exogenous GSH supplementation groups. The experimental data were analysed by a one-way ANOVA with post-hoc comparisons and  $p < 0.05$  was accepted as significant. The different uppercase letters in each column indicate significant differences between the NC groups. The different lowercase letters in each column indicates significant differences between the GSH groups. \* in each column indicates significant differences between the GSH group and the corresponding NC group.

As shown in our study, we identified the potential effect of GSH on the histone methylation modifications of ovine MII oocytes, as the expression levels of H3K4me3 in the Grade B-GSH and Grade C-GSH groups were significantly increased compared with those of the corresponding NC groups, which was consistent with the expression patterns of *Kdm4d* and *Kdm5b* in the Grade B-GSH and Grade C-GSH groups.

To date, the methylation of H3K4 and H3K9 has been widely studied, with accumulating evidence confirming the specific role of H3K4me3 during transcriptional activation and the specific role of H3K9me3 during the gene silencing process via the expression levels of KDM. Moreover, the demethylation process of H3K4me3 by the lysine demethylases of *Kdm5b* further regulated germline-inherited posttranslational histone modifications that promote ZGA and early mammalian embryonic development [26,59], which was consistent with our studies.

In the present study, we also found that the expression levels of H3K9me3 in the Grade B-GSH and Grade C-GSH groups were significantly enhanced after exogenous GSH supplementation. H3K9me3, regulated by the recruitment of DNA methyltransferase 3a (Dnmt3a), histone deacetylase 1 (HDAC1), histone methyltransferase G9a, heterochromatin protein 1 (HP1) and histone methyltransferase suppressor of variegation 3–9 homologue 1 (SUV39H1), has been identified as a crucial factor in defining oocyte developmental competence [60,61]. Furthermore, the overexpression of *Kdm4b* significantly ameliorated the defects of murine SCNT embryos, including increased boundaries of topologically associating domains (TADs) and abnormal superenhancer and promoter interactions caused by the inherited H3K9me3 [62]. In addition, Song et al. found that treatments with 7,12-dimethylbenz [a]anthracene (DMBA), an environmental pollutant, resulted in a significant decrease of H3K9me3, a higher incidence of DNA double strand breaks (DSBs) and early apoptosis in porcine COCs [63]. In striking contrast, none of these changes occurred in cumulus-denuded oocytes treated with DMBA, which further revealed the potential relationship between cumulus cells and histone methylations. However, the specific effects of exogenous GSH supplementation on the histone methylation process and the potential regulatory mechanism of ovine MII oocytes during IVM require further detailed investigations.

Taken together, our findings first provide a theoretical basis for the application of exogenous GSH to improve the *in vitro* developmental competence of ovine oocytes, especially oocytes matured from COCs lacking cumulus cells. We hope that this research will contribute to research related to GSH applications and the efficiency of ARTs for ovine breeding.

#### CRediT authorship contribution statement

**Jingyu Ren:** Data curation, Formal analysis, Investigation, Methodology. **Yuchun Hao:** Data curation, Investigation. **Zhanpeng Liu:** Data curation, Investigation. **Shubin Li:** Data curation, Investigation. **Chunyu Wang:** Data curation, Investigation. **Biao Wang:** Data curation, Funding acquisition, Investigation. **Yongbin Liu:** Data curation, Investigation. **Gang Liu:** Formal analysis, Funding acquisition, Investigation, Methodology, Resources, Supervision, Writing – original draft, Writing – review & editing. **Yanfeng Dai:** Funding acquisition, Project administration, Resources, Supervision.

#### Declaration of competing interest

The authors report no conflicts of interest in this work.

#### Acknowledgment

This work was supported by the National Natural Science Foundation of China (82060567 to Gang Liu), the Natural Science Foundation of Inner Mongolia (2020BS08014 to Gang Liu, 2017ZD04 to Yanfeng Dai), the Major science and technology projects of Inner Mongolia (2020ZD0003 to Yanfeng Dai) and the outstanding youth foundation of Inner Mongolia Academy of Agricultural & Animal Husbandry Sciences (2017QNJJM03 to Biao Wang).

#### Appendix A. Supplementary data

Supplementary data to this article can be found online at <https://doi.org/10.1016/j.theriogenology.2021.07.025>.

#### References

- [1] Galli C, Lazzari G. Practical aspects of IVM/IVF in cattle. *Animal Reproduction Science - ANIM REPROD SCI*. 1996;42:371–9.
- [2] Amiridis GS, Cseh S. Assisted reproductive technologies in the reproductive management of small ruminants. *Anim Reprod Sci* 2012;130:152–61.
- [3] Granleese T, Clark SA, Swan AA, van der Werf JH. Increased genetic gains in sheep, beef and dairy breeding programs from using female reproductive technologies combined with optimal contribution selection and genomic breeding values. *Genet Sel Evol : GSE*. 2015;47:70.
- [4] Niederberger C, Pellicer A, Cohen J, Gardner DK, Palermo GD, O'Neill CL, Chow S, Rosenwaks Z, Cobo A, Swain JE, Schoolcraft WB, Frydman R, Bishop LA, Aharon D, Gordon C, New E, Decherney A, Tan SL, Paulson RJ, Goldfarb JM, Brännström M, Donne J, Silber S, Dolmans M-M, Simpson JL, Handside AH, Munné S, Eguizabal C, Montserrat N, Izpisua Belmonte JC, Trounson A, Simon C, Tulandi T, Giudice LC, Norman RJ, Hsueh AJ, Sun Y, Laufer N, Kochman R, Eldar-Geva T, Lunenfeld B, Ezcurra D, D'Hooghe T, Fauser BCJM, Tarlatzis BC, Meldrum DR, Casper RF, Fatemi HM, Devroey P, Galliano D, Wikland M, Sigman M, Schoor RA, Goldstein M, Lipshultz LI, Schlegel PN, Hussein A, Oates RD, Brannigan RE, Ross HE, Pennings G, Klock SC, Brown S, Van Steirteghem A, Rebar RW, LaBarbera AR. Forty years of IVF. *Fertility and sterility*, vol. 110; 2018.
- [5] Sirard M-A. 40 years of bovine IVF in the new genomic selection context. *Reproduction* 2018;156:R1–7.
- [6] Brown HM, Dunning KR, Sutton-McDowall M, Gilchrist RB, Thompson JG, Russell DL. Failure to launch: aberrant cumulus gene expression during oocyte in vitro maturation. *Reproduction* 2017;153:R109–20.
- [7] Walter J, Huwiler F, Fortes C, Grossmann J, Roschitzki B, Hu J, Naegeli H, Laczko E, Bleul U. Analysis of the equine “cumulome” reveals major metabolic aberrations after maturation in vitro. *BMC Genom* 2019;20:588.
- [8] Liu Z, Ren Z, Zhang J, Chuang CC, Kandaswamy E, Zhou T, Zuo L. Role of ROS and nutritional antioxidants in human diseases. *Front Physiol* 2018;9:477.
- [9] Oyewole AO, Birch-Machin MA. Mitochondria-targeted antioxidants. *Faseb J : official publication of the Federation of American Societies for Experimental Biology* 2015;29:4766–71.
- [10] An Q, Peng W, Cheng Y, Lu Z, Zhou C, Zhang Y, Su J. Melatonin supplementation during in vitro maturation of oocyte enhances subsequent development of bovine cloned embryos. *J Cell Physiol* 2019;234:17370–81.
- [11] Devine PJ, Perreault SD, Luderer U. Roles of reactive oxygen species and antioxidants in ovarian toxicity. *Biol Reprod* 2012;86:27.
- [12] Seli E, Wang T, Horvath TL. Mitochondrial unfolded protein response: a stress response with implications for fertility and reproductive aging. *Fertil Steril* 2019;111:197–204.
- [13] Copley JN. Mechanisms of mitochondrial ROS production in assisted reproduction: the known, the unknown, and the intriguing, vol. 9. Basel, Switzerland: Antioxidants; 2020.
- [14] Lemire J, Alhasawi A, Appanna VP, Tharmalingam S, Appanna VD. Metabolic defence against oxidative stress: the road less travelled so far. *J Appl Microbiol* 2017;123:798–809.
- [15] Lushchak VI. Free radicals, reactive oxygen species, oxidative stress and its classification. *Chem Biol Interact* 2014;224:164–75.
- [16] Sasaki H, Hamatani T, Kamijo S, Iwai M, Kobanawa M, Ogawa S, Miyado K, Tanaka M. Impact of oxidative stress on age-associated decline in oocyte developmental competence. *Front Endocrinol* 2019;10:811.
- [17] Aitken RJ. Impact of oxidative stress on male and female germ cells: implications for fertility. *Reproduction* 2020;159:R189–201.
- [18] Agarwal A, Aponte-Mellado A, Premkumar BJ, Shaman A, Gupta S. The effects of oxidative stress on female reproduction: a review. *Reprod Biol Endocrinol : RBE (Rev Bras Entomol)* 2012;10:49.
- [19] Agarwal A, Gupta S, Sharma RK. Role of oxidative stress in female reproduction. *Reprod Biol Endocrinol : RBE (Rev Bras Entomol)* 2005;3:28.
- [20] Ding ZM, Jiao XF, Wu D, Zhang JY, Chen F, Wang YS, Huang CJ, Zhang SX, Li X, Huo LJ. Bisphenol AF negatively affects oocyte maturation of mouse in vitro

- through increasing oxidative stress and DNA damage. *Chem Biol Interact* 2017;278:222–9.
- [21] Eini F, Novin MG, Joharchi K, Hosseini A, Nazarian H, Piryaei A, Bidadkosh A. Intracytoplasmic oxidative stress reverses epigenetic modifications in polycystic ovary syndrome. *Reprod Fertil Dev* 2017;29:2313–23.
- [22] Zhu CC, Zhang Y, Duan X, Han J, Sun SC. Toxic effects of HT-2 toxin on mouse oocytes and its possible mechanisms. *Arch Toxicol* 2016;90:1495–505.
- [23] He YT, Wang W, Shen W, Sun QY, Yin S. Melatonin protects against Fenoxaprop-ethyl exposure-induced meiotic defects in mouse oocytes. *Toxicology* 2019;425:152241.
- [24] Meng F, Jiao XF, Chen F, Zhang XY, Duan ZQ, Ding ZM, Wu D, Wang YS, Zhang SX, Miao YL, Huo LJ. Isobutylparaben negatively affects porcine oocyte maturation through increasing oxidative stress and cytoskeletal abnormalities. *Environ Mol Mutagen* 2020;61:433–44.
- [25] Lord T, Martin JH, Aitken RJ. Accumulation of electrophilic aldehydes during postovulatory aging of mouse oocytes causes reduced fertility, oxidative stress, and apoptosis. *Biol Reprod* 2015;92:33.
- [26] Dahl JA, Jung I, Aanes H, Greggains GD, Manaf A, Lerdrup M, Li G, Kuan S, Li B, Lee AY, Preissl S, Jermstad I, Haugen MH, Suganthan R, Bjørås M, Hansen K, Dalen KT, Fedorcsak P, Ren B, Klungland A. Broad histone H3K4me3 domains in mouse oocytes modulate maternal-to-zygotic transition. *Nature* 2016;537:548–52.
- [27] Inoue A, Jiang L, Lu F, Suzuki T, Zhang Y. Maternal H3K27me3 controls DNA methylation-independent imprinting. *Nature* 2017;547:419–24.
- [28] Eckersley-Maslin MA, Alda-Catalinas C, Reik W. Dynamics of the epigenetic landscape during the maternal-to-zygotic transition. *Nat Rev Mol Cell Biol* 2018;19:436–50.
- [29] Sha QQ, Zhang J, Fan HY. Function and regulation of histone H3 lysine-4 methylation during oocyte meiosis and maternal-to-zygotic transition. *Frontiers in cell and developmental biology* 2020;8:597498.
- [30] Xing X, Zhang J, Wu T, Zhang J, Wang Y, Su J, Zhang Y. SIRT1 reduces epigenetic and non-epigenetic changes to maintain the quality of postovulatory aged oocytes in mice. *Exp Cell Res* 2021;399:112421.
- [31] Forman HJ, Zhang H, Rinna A. Glutathione: overview of its protective roles, measurement, and biosynthesis. *Mol Aspect Med* 2009;30:1–12.
- [32] Calabrese G, Morgan B, Riemer J. Mitochondrial glutathione: regulation and functions. *Antioxidants Redox Signal* 2017;27:1162–77.
- [33] de Matos DG, Furnus CC. The importance of having high glutathione (GSH) level after bovine in vitro maturation on embryo development effect of beta-mercaptoethanol, cysteine and cystine. *Theriogenology* 2000;53:761–71.
- [34] García-Martínez T, Vendrell-Flotats M, Martínez-Rodero I, Ordóñez-León EA, Álvarez-Rodríguez M, López-Béjar M, Yeste M, Mogas T. Glutathione ethyl ester protects in VitroMaturing bovine oocytes against oxidative stress induced by subsequent vitrification/warming. *Int J Mol Sci* 2020:21.
- [35] Kim IH, Van Langendonck A, Van Soom A, Vanroose G, Casi AL, Hendriksen PJ, Bevers MM. Effect of exogenous glutathione on the in vitro fertilization of bovine oocytes. *Theriogenology* 1999;52:537–47.
- [36] Zhou C, Zhang X, Chen Y, Liu X, Sun Y, Xiong B. Glutathione alleviates the cadmium exposure-caused porcine oocyte meiotic defects via eliminating the excessive ROS. *Environmental pollution (Barking, Essex : 1987)* 2019;255:113194.
- [37] Li F, Cui L, Yu D, Hao H, Liu Y, Zhao X, Pang Y, Zhu H, Du W. Exogenous glutathione improves intracellular glutathione synthesis via the  $\gamma$ -glutamyl cycle in bovine zygotes and cleavage embryos. *J Cell Physiol* 2019;234:7384–94.
- [38] Ledda S, Bogliolo L, Leoni G, Naitana S. Cell coupling and maturation-promoting factor activity in in vitro-matured prepubertal and adult sheep oocytes. *Biol Reprod* 2001;65:247–52.
- [39] Kelly JM, Kleemann DO, Rudiger SR, Walker SK. Effects of grade of oocyte-cumulus complex and the interactions between grades on the production of blastocysts in the cow, Ewe and lamb. *Reproduction in domestic animals = Zuchthygiene* 2007;42:577–82.
- [40] Mondal S, Mor A, Reddy IJ, Nandi S, Gupta PSP, Mishra A. In Vitro embryo production in sheep. *Methods in molecular biology*, vol. 2006; 2019. p. 131–40. Clifton, NJ.
- [41] Shirazi A, Shams-Esfandabadi N, Ahmadi E, Heidari B. Effects of growth hormone on nuclear maturation of ovine oocytes and subsequent embryo development. *Reproduction in domestic animals = Zuchthygiene* 2010;45:530–6.
- [42] Fidanza A, Toschi P, Zacchini F, Czernik M, Palmieri C, Scapolo P, Modlinski JA, Loi P, Ptak GE. Impaired placental vasculogenesis compromises the growth of sheep embryos developed in vitro. *Biol Reprod* 2014;91:21.
- [43] Santos L, Rodrigues B, Rodrigues J. In vitro nuclear maturation of bitch oocytes in the presence of polyvinyl-pyrrolidone. 2006.
- [44] Dai X, Qiu L, Zhao B, Gao Y, Mu Y, Chu Z, Du L, Xiong B. Melatonin ameliorates the fertilization capacity of oocytes exposed to 17 $\alpha$ -ethynylestradiol. *Reprod Toxicol* 2020;93:61–7.
- [45] Liu G, Li S, Yuan H, Hao M, Wurihan Yun Z, Zhao J, Ma Y, Dai Y. Effect of sodium alginate on mouse ovary vitrification. *Theriogenology* 2018;113:78–84.
- [46] Zhou C, Zhang X, Chen Y, Liu X, Sun Y, Xiong B. Glutathione alleviates the cadmium exposure-caused porcine oocyte meiotic defects via eliminating the excessive ROS. *Environmental pollution (Barking, Essex : 1987)* 2019;255:113194.
- [47] Zhang M, ShiYang X, Zhang Y, Miao Y, Chen Y, Cui Z, Xiong B. Coenzyme Q10 ameliorates the quality of postovulatory aged oocytes by suppressing DNA damage and apoptosis. *Free Radical Biol Med* 2019;143:84–94.
- [48] Miao Y, Zhou C, Cui Z, Zhang M, ShiYang X, Lu Y, Xiong B. Postovulatory aging causes the deterioration of porcine oocytes via induction of oxidative stress. *Faseb J : official publication of the Federation of American Societies for Experimental Biology* 2018;32:1328–37.
- [49] Hosoe M, Shioya Y. Distribution of cortical granules in bovine oocytes classified by cumulus complex. *Zygote* 1997;5:371–6.
- [50] Ackert CL, Gittens JE, O'Brien MJ, Eppig JJ, Kidder GM. Intercellular communication via connexin43 gap junctions is required for ovarian folliculogenesis in the mouse. *Dev Biol* 2001;233:258–70.
- [51] Miao Y, Cui Z, Gao Q, Rui R, Xiong B. Nicotinamide mononucleotide supplementation reverses the declining quality of maternally aged oocytes. *Cell Rep* 2020;32:107987.
- [52] Dai X, Lu Y, Zhang M, Miao Y, Zhou C, Cui Z, Xiong B. Melatonin improves the fertilization ability of post-ovulatory aged mouse oocytes by stabilizing ovastacin and Juno to promote sperm binding and fusion. *Hum Reprod* 2017;32:598–606.
- [53] Burkart AD, Xiong B, Baibakov B, Jiménez-Movilla M, Dean J. Ovastacin, a cortical granule protease, cleaves ZP2 in the zona pellucida to prevent polyspermy. *J Cell Biol* 2012;197:37–44.
- [54] Zhang M, Dai X, Lu Y, Miao Y, Zhou C, Cui Z, Liu H, Xiong B. Melatonin protects oocyte quality from Bisphenol A-induced deterioration in the mouse. *J Pineal Res* 2017;62.
- [55] Marcho C, Cui W, Mager J. Epigenetic dynamics during preimplantation development. *Reproduction* 2015;150:R109–20.
- [56] Sepulveda-Rincon LP, Solanas Edel L, Serrano-Revuelta E, Ruddick L, Maalouf WE, Beaujean N. Early epigenetic reprogramming in fertilized, cloned, and parthenogenetic embryos. *Theriogenology* 2016;86:91–8.
- [57] Yu XX, Liu YH, Liu XM, Wang PC, Liu S, Miao JK, Du ZQ, Yang CX. Ascorbic acid induces global epigenetic reprogramming to promote meiotic maturation and developmental competence of porcine oocytes. *Sci Rep* 2018;8:6132.
- [58] Thuy Van NT, Anh My LB, Van Thuan N, Bui HT. Improve the developmental competence of porcine oocytes from small antral follicles by pre-maturation culture method. *Theriogenology* 2020;149:139–48.
- [59] Sankar A, Lerdrup M, Manaf A, Johansen JV, Gonzalez JM, Borup R, Blanshard R, Klungland A, Hansen K, Andersen CY, Dahl JA, Helin K, Hoffmann ER. KDM4A regulates the maternal-to-zygotic transition by protecting broad H3K4me3 domains from H3K9me3 invasion in oocytes. *Nat Cell Biol* 2020;22:380–8.
- [60] Russo V, Bernabò N, Di Giacinto O, Martelli A, Mauro A, Berardinelli P, Curini V, Nardinocchi D, Mattioli M, Barboni B. H3K9 trimethylation precedes DNA methylation during sheep oogenesis: HDAC1, SUV39H1, G9a, HP1, and Dnmts are involved in these epigenetic events. *J Histochem Cytochem : official journal of the Histochemistry Society* 2013;61:75–89.
- [61] Canovas S, Ross PJ. Epigenetics in preimplantation mammalian development. *Theriogenology* 2016;86:69–79.
- [62] Chen M, Zhu Q, Li C, Kou X, Zhao Y, Li Y, Xu R, Yang L, Yang L, Gu L, Wang H, Liu X, Jiang C, Gao S. Chromatin architecture reorganization in murine somatic cell nuclear transfer embryos. *Nat Commun* 2020;11:1813.
- [63] Song ZQ, Li X, Wang YK, Du ZQ, Yang CX. DMBA acts on cumulus cells to desynchronize nuclear and cytoplasmic maturation of pig oocytes. *Sci Rep* 2017;7:1687.